

## 論文内容の要旨

論文題目  $\pi$ -Conjugated Metalladithiolenes: Developments toward  
Two-Dimensional Nanosheets  
( $\pi$ 共役メタラジチオレン錯体の二次元ナノシートへの展開)

氏名 神戸 徹也

### [Introduction]

Bottom-up fabrication of microscopic and mesoscopic materials with sizes between molecules and bulk materials is a challenging research target. In this research field, supramolecular structures comprising metal complexes such as coordination polymers and metal clusters have attracted much attention, because they provide several unique functionalities derived from hybridization between transition metals and organic ligands.

Metalladithiolene is one of the best components for functional molecular systems because of its unique properties and reactivities. Focusing on its attractive electronic structure, our laboratory has developed the research of metalladithiolene chemistry from the viewpoint of multi-nucleation.

The aim of my Ph. D. research is to develop a new strategy for design and synthesis of  $\pi$ -conjugated multi-nuclear metal complexes. As the first step, I expanded the family of the  $\pi$ -conjugated trinuclear metalladithiolene complexes with use of planar bridging ligands. I also developed a two-dimensional nanosheet by the extension of the trinuclear complexes. Their physical properties were also investigated.

## [Trinuclear Metalladithiolene Complexes Bridged by Arenes]

Trinuclear metalladithiolene complexes with group 9 metals (Co, Rh and Ir) were developed in my laboratory. Here I have expanded the variation of the metal center to groups 8 (Ru; **1**) and 10 (Ni and Pt; **2** and **3**), and investigated the mixed-valence states of trinuclear metalladithiolene complexes **1-6** (Figure 1).

**1** and **2** exhibit intense electronic communication through the phenylene bridge among the three dithiolene moieties upon oxidation, which was not confirmed in the group-9 complexes. **3** exhibits an intense absorption band across the visible and NIR regions, which is assigned as a charge-transfer-to-diimine electronic band. This band is red-shifted and broadened compared to its corresponding mononuclear complex.

Triphenylene-bridged complexes **4-6** also possess inter-metal interaction which creates mixed-valent states. This behavior was disclosed by electrochemical and spectroscopic measurements. Their differential pulse voltammograms can be assigned to three-step one-electron reductions, and an inter valence charge transfer band has also been observed during the chemical reduction process.

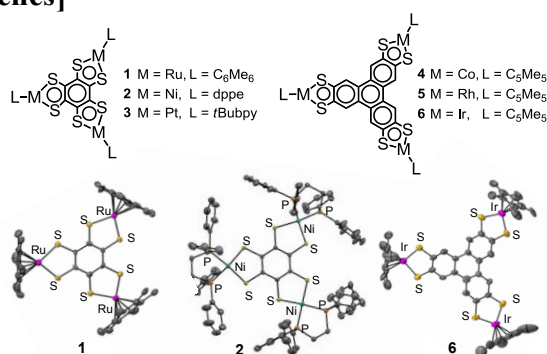


Figure 1.  $\pi$ -conjugated metalladithiolenes: Trinuclear complexes with phenylene (**1-3**) and triphenylene (**4-6**) bridging units, and their crystal structures (**1**, **2** and **6**). dppe = 1,2-Bis(diphenylphosphino)ethane, bpy = 2,2'-bipyridine.

## [ $\pi$ -Conjugated Metalladithiolene Nanosheet]

The  $\pi$ -conjugated trinuclear complexes noted above lead to the formation of two-dimensional  $\pi$ -conjugated nanosheet structures with the features of metalladithiolenes such as a planar skeleton, aromatic structure, and redox activity (Figure 2).

$\pi$ -conjugated nanosheets have attracted massive attention of scientists since the discovery of graphene. Graphene demonstrates unique physical and chemical properties such as high carrier mobilities and unconventional quantum hall effect. Metalladithiolene nanosheet **7** features  $\pi$ -conjugation spread over the whole sheet, thereby being expected to possess unique properties. Nanosheet **7** can be a potential revolutionary nanomaterial.

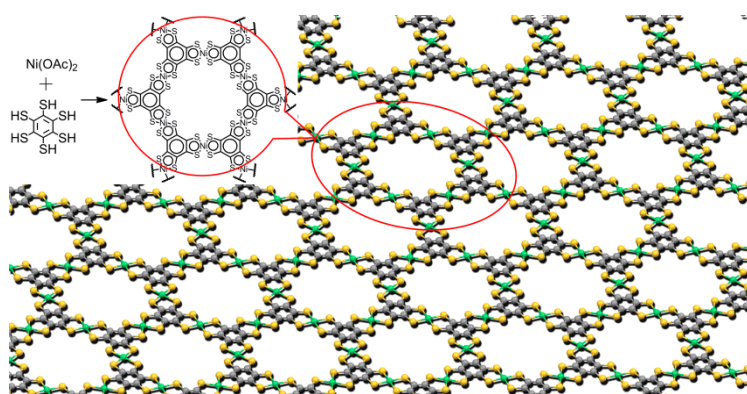


Figure 2. Illustration and chemical structure of a single layer nickelladithiolene nanosheet (**7**)

## [Fabrication, Identification and Fundamental Properties of the Nickelladithiolene Nanosheet]

A liquid-liquid interfacial synthesis using a dichloromethane solution of benzenehexathiophene (BHT) and aqueous solution of Ni(OAc)<sub>2</sub> gave stacked nickelladithiolene nanosheet **7** at the interface as a black film with metallic luster (Figure 3a). A scanning electron microscopy (SEM) image shows a sheet-like

structure with a high aspect ratio (Figure 3b). The thickness of the stacked nanosheet is 1  $\mu\text{m}$ , corresponding to several thousand layers. A transmission electron microscopy (TEM) image around the edge of the nanosheet exhibits a layered structure, and electron diffractions in this area correspond to a hexagonal pattern with an in-plane periodicity of 1.4-1.5 nm (Figure 3c). The structure was determined precisely with a powder X-ray diffraction (PXRD) measurement using a synchrotron radiation: Stacked **7** was revealed to have a staggered stacked structure (Figure 3d).

An atomically thin nanosheet was obtained using a modified synthetic procedure. An ethyl acetate solution of BHT was sparged on the surface of an aqueous nickel solution to fabricate a thin nanosheet at the gas-liquid interface. The atomically thin nanosheet was transferred on a substrate using the Langmuir-Schäfer method. The sample on HOPG was analyzed using scanning probe microscopy (SPM) to determine its structure. An atomic force microscopy (AFM) image shows a flat sheet structure with a thickness of 0.6 nm (Figure 3e). This nanosheet is assigned as a single layer, judging from the observable thickness of single-layered graphene on a silicon substrate (0.5-1 nm). A scanning tunneling microscopy (STM) image gives a hexagonal ordered structure (Figure 3f). The periodicity of the ordered structure (4.9 nm) is greater than expected from the result of PXRD (1.41 nm). This discrepancy stems from moiré interference between the nanosheet and HOPG lattice.

A cyclic voltammograms for **7** prepared by a 25-time deposition of the single-layered nanosheet on an HOPG substrate as a working electrode show a reversible redox wave at 0.21 V (vs.  $\text{Fc}^+/\text{Fc}$ ), derived from the bis(dithiolene) moiety with  $-1$  and  $0$  oxidation states (Figure 3g). These two oxidation states contribute to the mixed-valence state of **7**. The oxidation states were determined by means of X-ray photoelectron spectroscopy (XPS) focusing on the S 2s region.

The ratio between  $-1$  and  $0$  was found to be 74 : 26.

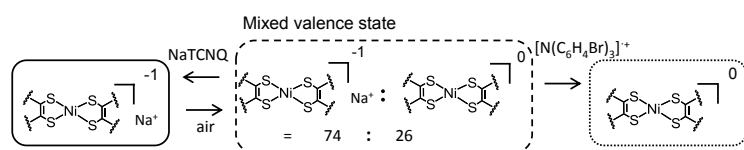


Figure 4. Schematic illustration of the chemical change of the oxidation states.

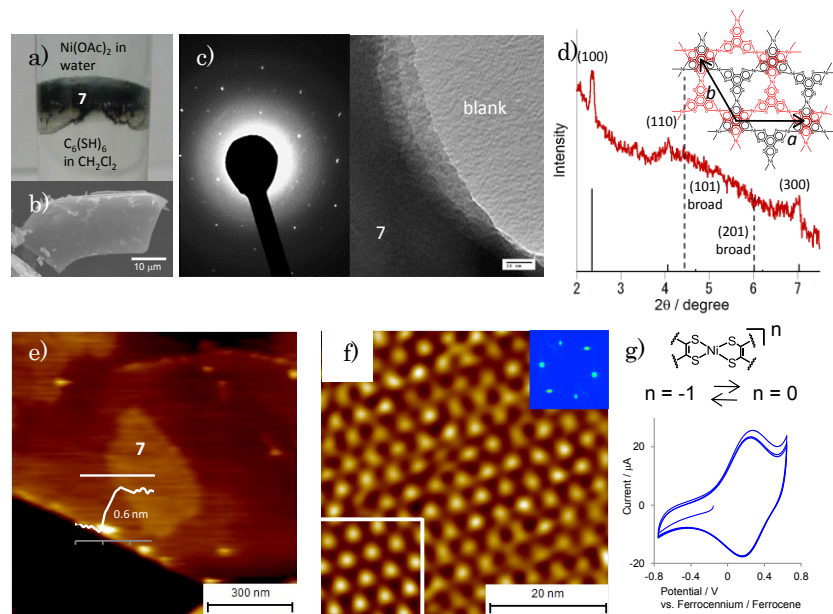


Figure 3. (a) Photograph of stacked **7** at the interface. (b) SEM image (c) Selected area electron diffraction and TEM image. (d) Experimental (top) and simulated (bottom) PXRD. (e) AFM height image and its cross-section analysis of a single-layer **7**. (f) STM height image of a single-layer **7** showing the hexagonal pattern. The insets at the upper right and left lower are FFT and FFT-filtered image, respectively. (g) Cyclic voltammogram of **7** on HOPG in 1 M  $\text{Bu}_4\text{NClO}_4\text{-CH}_2\text{Cl}_2$ .

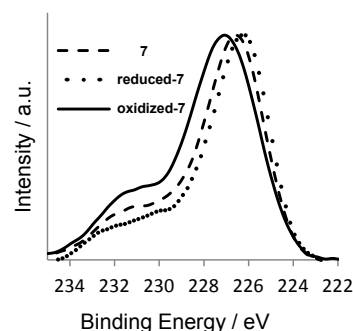


Figure 5. Schematic illustration of the chemical change of the oxidation states.

## [Modulation of the Electronic State of $\pi$ -Conjugated Nickelladithiolenes Complex Nanosheet]

Chemical reduction of as-prepared **7** with a sodium salt of 7,7,8,8-tetracyanoquinonodimethane anion radical (NaTCNQ) gives rise to **reduced-7**, where all the nickelladithiolenes units take the  $-1$  oxidation state. On the other hand, a reaction between **7** and tris(4-bromophenyl)ammoniumyl cation radical yields **oxidized-7**, where all nickelladithiolenes units take the  $0$  oxidation state (Figure 4). Their oxidation states were determined by the binding energy of the S 2s peak in XPS (Figure 5). Furthermore, the peaks near the Fermi energy in photoemission spectroscopy move according to the change in the oxidation state, which indicates a shift of the Fermi level. These results demonstrate that the electron doping can be tuned by chemical control of the oxidation state.

The change in the electronic state triggers tuning of properties. The electro-conductivities of stacked **7** and **oxidized-7** were measured using the van der Pauw method. Stacked **oxidized-7** shows the highest conductivity ( $38 \text{ Scm}^{-1}$ ) among them. It decreased according to a temperature fall with two activation energies of  $10 \text{ meV}$  ( $> 80\text{K}$ ) and  $2 \text{ meV}$  ( $< 80\text{K}$ ).

## [Variation of metal complex nanosheets]

The series of metal complex nanosheets are expanded by changing counter cations, metal centers and bridging ligands (Figure 6). Large and planar cations of  $\text{Bu}_4\text{N}^+$  and  $\text{BMI}^+$  are introduced instead of  $\text{Na}^+$  in **7**, which leads to the change of electronic conductivity.

$\text{Pd(II)}$  is adapted for the metalladithiolenes nanosheet. Interfacial reactions with use of oxidizing agent ( $\text{K}_3\text{Fe(CN)}_6$ ) gives Palladium bis(dithiolenes) nanosheet without the formation of reduced Pd nanoparticles. I also investigated Nickel bis(diaminoate) nanosheet with triphenylene bridging skeleton, which is expected to have different electronic properties from bis(dithiolenes) nanosheet **7**.

## [Conclusions]

In the series of research, the family of trinuclear metalladithiolenes complexes was successfully expanded, and the first step was made towards the development of metalladithiolenes two-dimensional structures. Stacked and atomically thin metalladithiolenes nanosheets (**7**) have been fabricated from the liquid-liquid and the gas-liquid interfaces. The structure, composition, and properties of **7** were identified comprehensively using PXRD, XPS, SEM, HR-TEM, IR spectroscopy, elemental analysis, electrochemical measurements, and SPM measurements. Electronic doping was achieved through the control of the oxidation states by chemical reduction and oxidation reactions, which afforded the modulation of its electronic states and properties without affecting its structure. The series of  $\pi$ -conjugated metal complex nanosheets are fabricated using wide variations of the counter cations, metal centers and bridging ligands.

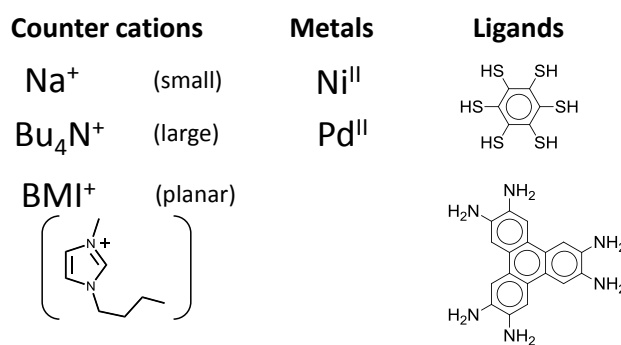


Figure 6. Variations of the components of metal complex nanosheet (Counter cations, Metal centers and bridging ligands).